Imaging, Diagnosis, Prognosis
See commentary by Shields, p. 1189

Clinical Cancer Research

[^{18}F]FLT–PET Imaging Does Not Always "Light Up" Proliferating Tumor Cells

Cathy C. Zhang[1], Zhengming Yan[1], Wenlin Li[3], Kyle Kuszpit[2], Cory L. Painter[1], Qin Zhang[1], Patrick B. Lappin[5], Tim Nichols[5], Maruja E. Lira[1], Timothy Affolter[5], Neeta R. Fahey[4], Carleen Cullinane[6], Mary Spilker[3], Kenneth Zasadny[2], Peter O'Brien[3], Dana Buckman[1], Anthony Wong[5], and James G. Christensen[1]

Abstract

Purpose: [^{18}F]FLT (3′-Fluoro-3′ deoxythymidine)–PET imaging was proposed as a tool for measuring *in vivo* tumor cell proliferation. The aim of this article was to validate the use of [^{18}F]FLT–PET imaging for measuring xenograft proliferation and subsequent monitoring of targeted therapy.

Experimental Design: In exponentially growing xenografts, factors that could impact the outcome of [^{18}F]FLT–PET imaging, such as nucleoside transporters, thymidine kinase 1, the relative contribution of DNA salvage pathway, and the ratio of FLT to thymidine, were evaluated. The [^{18}F]FLT tracer avidity was compared with other proliferation markers.

Results: In a panel of proliferating xenografts, [^{18}F]FLT or [^{3}H]thymidine tracer avidity failed to reflect the tumor growth rate across different tumor types, despite the high expressions of Ki67 and TK1. When FLT was injected at the same dose level as used in the preclinical [^{18}F]FLT–PET imaging, the plasma exposure ratio of FLT to thymidine was approximately 1:200. Thymidine levels in different tumor types seemed to be variable and exhibited an inverse relationship with the FLT tracer avidity. In contrast, high-dose administration of bromdeoxyuridine (BrdUrd; 50 mg/kg) yielded a plasma exposure of more than 4-fold higher than thymidine and leads to a strong correlation between the BrdUrd uptake and the tumor proliferation rate. In FLT tracer-avid models, [^{18}F]FLT–PET imaging as a surrogate biomarker predicted the therapeutic response of CDK4/6 inhibitor PD-0332991.

Conclusions: Tumor thymidine level is one of the factors that impact the correlation between [^{18}F]FLT uptake and tumor cell proliferation. With careful validation, [^{18}F]FLT–PET imaging can be used to monitor antiproliferative therapies in tracer-avid malignancies. *Clin Cancer Res; 18(5); 1303–12. ©2011 AACR.*

Introduction

In 1998, Shields and colleagues introduced [^{18}F]FLT (3′-Fluoro-3′ deoxythymidine)–PET imaging as a noninvasive tool for visualizing tumor cell proliferation (1). Since then, the technology has attracted substantial attention for its various applications in oncology. The principal mechanism in [^{18}F]FLT–PET imaging (2) is the uptake of the tracer by proliferating cells in the pyrimidine salvage pathway, mostly during S-phase. The tracer is then phosphorylated by thymidine kinase 1 (TK1), at which point it becomes trapped in the cells. As a pyrimidine analog, FLT primarily relies on the pyrimidine transporters, including equilibrative nucleoside transporters 1 and 2 (ENT1 and 2) and concentrative nucleoside transporters 1 and 3 (CNT1 and 3), to enter cells prior to being phosphorylated (3, 4). Using a cell-based assay, FLT retention in cells was found to be strongly associated with TK1 expression (5). In some cases, tumor cells predominately synthesize the nucleosides that are needed for cell growth *de novo* (6), which results in low [^{18}F]FLT tracer avidity in the proliferating tumor, leading to false negative results (7, 8). Clearly, in order for [^{18}F]FLT–PET imaging to "light up" proliferating cells, a number of factors must come into play. This may explain why clinical [^{18}F]FLT–PET imaging exhibited lower overall uptake and less specificity compared with [^{18}F] FDG–PET imaging, despite being a more favorable tool for visualizing malignant tissues. Therefore, [^{18}F]FLT–PET imaging is less appropriate for clinical tumor staging (9).

Because antiproliferation is often a primary or secondary phenotypic change caused by cytotoxic and targeted therapy, [^{18}F]FLT–PET imaging seemed to be a comparatively straight-forward approach for tracking therapeutic-

Authors' Affiliations: [1]Oncology Research Unit, [2]Bio-Imaging Unit, La Jolla Laboratories, Pfizer Global Research and Development, San Diego, California; [3]Pharmacokinetics, Dynamics & Metabolism, [4]Molecular Medicine, Groton Laboratories, Pfizer Global Research and Development, Groton, Connecticut; [5]Drug Safety Research & Development, Pfizer Global Research and Development, New York, New York; and [6]Centre for Molecular Imaging and Translational Research Laboratory, Peter MacCallum Cancer Centre, East Melbourne, Victoria, Australia

Note: Supplementary data for this article are available at Clinical Cancer Research Online (http://clincancerres.aacrjournals.org/).

Corresponding Author: Cathy C. Zhang, Oncology Research Unit, Pfizer Global Research and Development, 10724 Science Center Road, San Diego, CA 92121. Phone: 858-622-3125; Fax: 858-622-5999; E-mail: cathy.zhang@pfizer.com

doi: 10.1158/1078-0432.CCR-11-1433

Translational Relevance

[^{18}F]FLT (3′-Fluoro-3′ deoxythymidine)–PET imaging has been employed to measure *in vivo* tumor cell proliferation; however, its use in clinical tumor staging is limited due to the lower overall uptake of FLT. In this article, we assessed the translational aspects of the [^{18}F]FLT–PET imaging modality with various assays and technologies to evaluate factors other than tumor cell proliferation that could impact the outcome of imaging. By selecting tracer-avid malignancies, the preclinical use of [^{18}F]FLT–PET imaging for tracking therapeutic response was also evaluated. The results of this study strongly agreed with the clinical outcome. This work highlights the preclinical understanding of [^{18}F]FLT–PET imaging and provides insights into the strengths and weaknesses of the technology applications in the oncology arena.

associated cell-cycle arrest before morphologic changes become measurable (10). In comparison, the conventional biopsy approach used in proof of mechanism studies is generally invasive and often shows histopathologic heterogeneity. In this respect, translational imaging research has been considerably emphasized for correlating [^{18}F]FLT–PET imaging readouts with target biomarker changes that are measured by other tools in the preclinical and clinical arenas. A number of preclinical [^{18}F]FLT–PET translational imaging studies have reported using early investigative anticancer agents, including the MAP/ERK kinase inhibitor PD-0325901 (11), the epidermal growth factor receptor (EGFR) inhibitor erlotinib (12), the mTOR inhibitor everolimus (13), the P-cadherin antibody PF-03732010 (14), and the aurora B kinase inhibitor AZD1152 (7). Using the tumor models that are responding to therapy, these reports showed that treatment-induced modulation of the targets is closely associated with a decline in [^{18}F]FLT retention. In all of the above cases, the decrease in [^{18}F]FLT uptake was linked with suppression of the proliferation marker Ki67. In the clinical setting, [^{18}F]FLT–PET imaging led to early detection of a therapeutic response to the EGFR inhibitor gefitinib in advanced lung adenocarcinoma (15). The robust inhibition of CDK4/6 enzymatic activity by PD-0332991 (16) resulted in a significant decrease in [^{18}F]FLT retention in recurrent mantle cell lymphoma patients at early disease stage (17). The [^{18}F]FLT–PET imaging outcome was correlated with the histologic readout of Rb hypophosphorylation, which is indicative of CDK4/6 inhibition.

In an attempt to find an alternative tool for measuring the uptake of an FLT tracer in tumors, Wenlin Li and colleagues (18) developed a liquid chromatography/mass spectrometry (LC/MS) method to test the level of FLT-MP (monophosphate) in tissues. During [^{18}F]FLT–PET imaging process (2 hours), 50% or more of the injected FLT is present in tumor cells as FLT-MP (19). Therefore, the FLT-MP amount is predicted to proportionally reflect the [^{18}F]FLT–PET imaging output. The advantage of this LC/MS method is that in addition to monitoring the uptake of the [^{18}F]FLT tracer, we can simultaneously measure FLT kinetics and distribution, as well as the level of thymidine in the tumor, thereby providing insight into the oncology application for [^{18}F]FLT–PET imaging technology.

The initial aim of our research was to evaluate the preclinical use of [^{18}F]FLT–PET imaging as a surrogate endpoint for measuring a targeted response. However, the models we tested that had the ideal molecular background did not always "light up" during proliferating state. This situation was also true in the clinical setting during the recruitment for multiple phase I trials for Pfizer early development drug candidates. The malignancies present in some patients do not exhibit enough tracer avidity to allow the measurable changes after therapeutic intervention. In this article, we address several key questions about the translational aspect of this imaging technology. First, do all growing tumors exhibit avidity for [^{18}F]FLT tracer? Second, are there factors other than induction of therapy that impact [^{18}F]FLT–PET imaging outcome? Last, what is the optimal strategy for utilizing [^{18}F]FLT–PET imaging as a surrogate biomarker to monitor therapy?

Materials and Methods

PD-0332991 was synthesized by chemists at Pfizer (16). Unless otherwise noted, all cell lines and fine chemicals were purchased from American Type Culture Collection and Sigma-Aldrich, respectively. MDA-MB-231Luc was purchased from Xenogen (Caliper Company). MDA-MB-231R was established by continuous exposure of MDA-MB-231 cells to taxol (20 nmol/L). The antibodies used were anti-Ki67 (Lab Vision), anti-BrdUrd (bromodeoxyuridine; BD Pharmingen), anti-Human TK 1 (Abcam), and anti-phospho-Rb (Ser780; Santa Cruz).

In vitro assays

Cell-cycle analysis was done with a fluorescence-activated cell sorting (FACS) Calibur system (Becton-Dickinson) using the CycleTEST Plus Kit (Becton-Dickinson). The mRNA expression levels of the nucleoside transporters were assessed by using the RNeasy Kit (Qiagen) on an ABI Prism 7900 (Applied Biosystems). The mRNA expression levels of the nucleotide transporters were assessed by reverse-transcription PCR (RT-PCR) using ABI Prism 7900 (Applied Biosystems). Total RNA was isolated using RNeasy Kit (Qiagen). The RNA concentration and quality was assessed using nanoDrop (Thermo-Scientific) and 2100 Bioanalyzer (Agilent), respectively. The cDNA was synthesized using cDNA high-capacity RT Kit (Applied Biosystems) and amplified real time using TaqMan assays for human CNT1-3 and ENT1-4 (Applied Biosystems). The expression levels were normalized to endogenous glyceraldehydes-3-phosphate dehydrogenase (GAPDH). For the *in vitro* FLT uptake test, tumor cells in the exponential growth stage were cultured with 100 nmol/L FLT in the presence and absence

of 1 μmol/L thymidine. After 2 hours, the medium was removed and the cells were washed with ice-cold PBS.

LC/MS analysis of FLT, thymidine, FLT-MP, and BrdUrd

FLT, thymidine, BrdUrd, and FLT-MP concentrations were analyzed as described previously (18) using the Sciex API 4000 Mass Spectrometer (Applied Biosystems). Tumors or cell pellets were precipitated with methanol. The supernatant (20 μL) was injected onto a 100 × 2 mm/Aqua C18 column (Phenomenex) and eluted with a linear gradient of 0.1% formic acid: 0.1% formic acid in acetonitrile from 100:0 to 20:80 for more than 5 minutes at a flow rate of 0.4 mL/min.

In vivo studies and drug administration

All experimental animal procedures complied with the Guide for the Care and Use of Laboratory Animals (Institute for Laboratory Animal Research, 1996) and were approved by the Pfizer Global Research and Development Institutional Animal Care and Use Committee. Two million cells were implanted in the dorsal region of athymic NCr-nu/nu or severe combined immunodeficient-beige mice (Charles River Breeding Laboratories). For *in vivo* thymidine delivery, subcutaneous implantation of a loaded miniosmotic pump (1003D, Alzet) was done following the manufacturer's instructions. Tumor growth rate was calculated as reported previously (20). To evaluate efficacy, mice were randomly assigned to 2 groups when tumors reached a volume of 150 to 200mm^3, such that the mean value of tumor size was identical between the groups. Vehicle or PD-0332991 (150 mg/kg) was perorally administered to mice once daily for 14 days. Tumor growth inhibition (TGI; ref. 21) was calculated after treatment was ended.

Pharmacokinetic and pharmacodynamic analyses

For pharmacokinetic analysis of FLT (2 μg/kg) and BrdUrd (50 mg/kg), tracer was administered to mice intravenously and intraperitoneally, respectively, prior to retroorbital bleed. Plasma levels were obtained at 0.25, 0.5, 1.5, and 2 hours. Tracer exposure [area under the curve (AUC_{0-2h})] value was calculated using the noncompartmental model of WinNonlin Professional Software version 4.0.1 (Pharsight). The assessment of pharmacodynamic endpoints was done using [18F]FLT–PET scan and LC/MS analysis for FLT-MP levels. Immunohistochemical (IHC) analyses of proliferation markers were carried out during the exponential growth stage of the tumors, while tumors were in the range of 200 to 600 mm^3. Data for each PD assessment were derived from a minimum of 5 tumor-bearing mice.

Immunohistochemical staining

Tumor samples were collected and prepared into formalin-fixed, paraffin-embedded tissue blocks. The staining procedure was carried out according to the manufacturer's protocol. The intensity of IHC staining was semiquantitatively scored on a scale of 0 to 4 by board-certified pathologists. Further quantification of the IHC staining, in multiple naive xenograft models, was done using a Vectra automated slide scanner (Cambridge Research and Instrumentation/Caliper). The CRI's Inform image analysis software allowed the quantification of % positivity from viable portions of the xenograft.

[18F]FLT–PET imaging

Preclinical [18F]FLT–PET and CT imaging was done using a microPET Focus F220 scanner (Siemens Medical Solutions) and a GE eXplore microCT scanner (GE Healthcare), respectively, as described previously (21). Tumor-bearing mice were anesthetized and administered 250 μCi (1–2 μg/kg) of [18F]FLT tracer intravenously. After 60 to 80 minutes, PET imaging was initiated, followed by a subsequent CT scan (5 minutes) for anatomical reference. The imaging process was finished within 2 hours of the tracer injection. Reconstructed PET and CT data were coregistered and volumes of interest were hand drawn to fit the primary tumor according to the CT and PET data sets. The standardized uptake value (SUV) was calculated using the following formula:

$$\mathrm{SUV} = C_{PET}(T)/(ID/W)$$

In which C_{PET} is the measured activity in the volume of interest, ID is the injected dose (μCi), and W is the mouse body weight. In this article, [18F]FLT uptake in xenografts was reported as a ratio of SUV (tumor SUV_{max}/liver SUV_{mean}) activity (22, 23), obtained by using the SUV of the most intense pixel in the tumor regions and normalized with the corresponding liver SUV_{mean} value from the same mouse.

Results

Variable [18F]FLT tracer uptake in xenograft models

To utilize [18F]FLT–PET imaging as a surrogate biomarker in the proof of mechanism studies, tumor models with high tracer avidity were chosen, providing a high enough signal to allow for adequate evaluation of treatment-induced decrease in signal. In a panel of nontreated xenograft models, [18F]FLT–PET imaging was done when tumors were in the exponential growth stage. Tracer uptake was assessed by calculating the tumor-to-liver SUV ratio (Fig. 1). We have observed variable [18F]FLT tracer uptake by different xenografts.

The relationship between tumor growth rate and [18F]FLT tracer avidity in xenograft models

To understand the correlation between tumor growth rate and FLT tracer avidity in the preclinical setting, [18F]FLT–PET imaging was done in a panel of xenograft models. In addition, FLT uptake was tested using LC/MS analysis for FLT-MP levels in separate cohorts of tumor-bearing mice. Figure 2A depicts the representative [18F]FLT–PET images of the tested tumor models. Quantitative assessments showed that the tumor growth rate was not reflected by the FLT tracer avidity, which was measured by either [18F]FLT uptake via PET imaging (Fig. 2B) or FLT-MP levels via LC/MS analyses. In these tumor models, we observed a

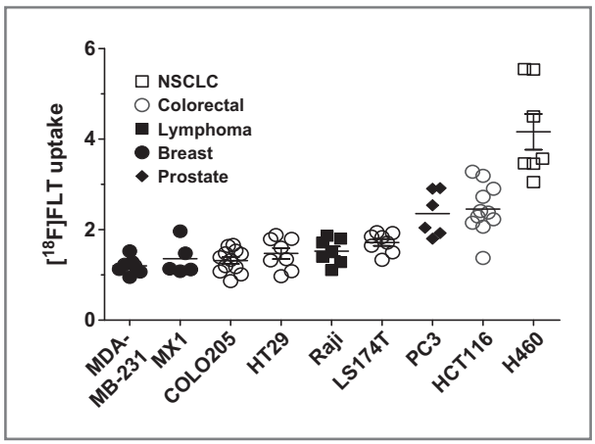

Figure 1. [^{18}F]FLT–PET imaging measurement of [^{18}F]FLT tracer avidity in multiple exponentially growing xenografts. [^{18}F]FLT uptake = SUV ratio (tumor SUV_{max}/liver SUV_{mean}). NSCLC, non–small cell lung carcinoma.

linear correlation (Fig. 2C) between the [^{18}F]FLT uptake and FLT-MP levels ($R^2 = 0.99$). These results suggested that the measurement of FLT-MP levels can be used as an alternative tool for measuring FLT tracer uptake. To confirm that the [^{18}F]FLT uptake truly reflect the thymidine uptake during DNA salvage pathway, we carried out [^{3}H]thymidine uptake assay in a selected panel of tumor models (Supplementary Fig. S1). The results showed a strong correlation between the [^{18}F]FLT tracer avidity and [^{3}H]thymidine uptake. Interestingly, the MDA-MB-231, MDA-MB-231Luc, and MDA-MB-231R tumor models exhibited different growth rates and [^{18}F]FLT uptakes, despite being derived from the same line.

The correlation of tumor growth and histologic markers of proliferation in xenograft models

Histologic analyses of multiple proliferation markers, including BrdUrd, Ki67, and TK1, were done in xenografts that were in the exponential growth stage. Among these markers, BrdUrd uptake and Ki67 are two established measures of proliferation. Tumor-bearing mice were administered BrdUrd (50 mg/kg) intraperitoneally. Tumors were harvested after 2 hours. Quantitative histologic analysis of IHC positivity was carried out using the CRI imaging system. In the tested xenograft models, the percentage of positively stained BrdUrd cells exhibited a positive linear correlation ($R^2 = 0.80$) with the tumor growth rate, whereas

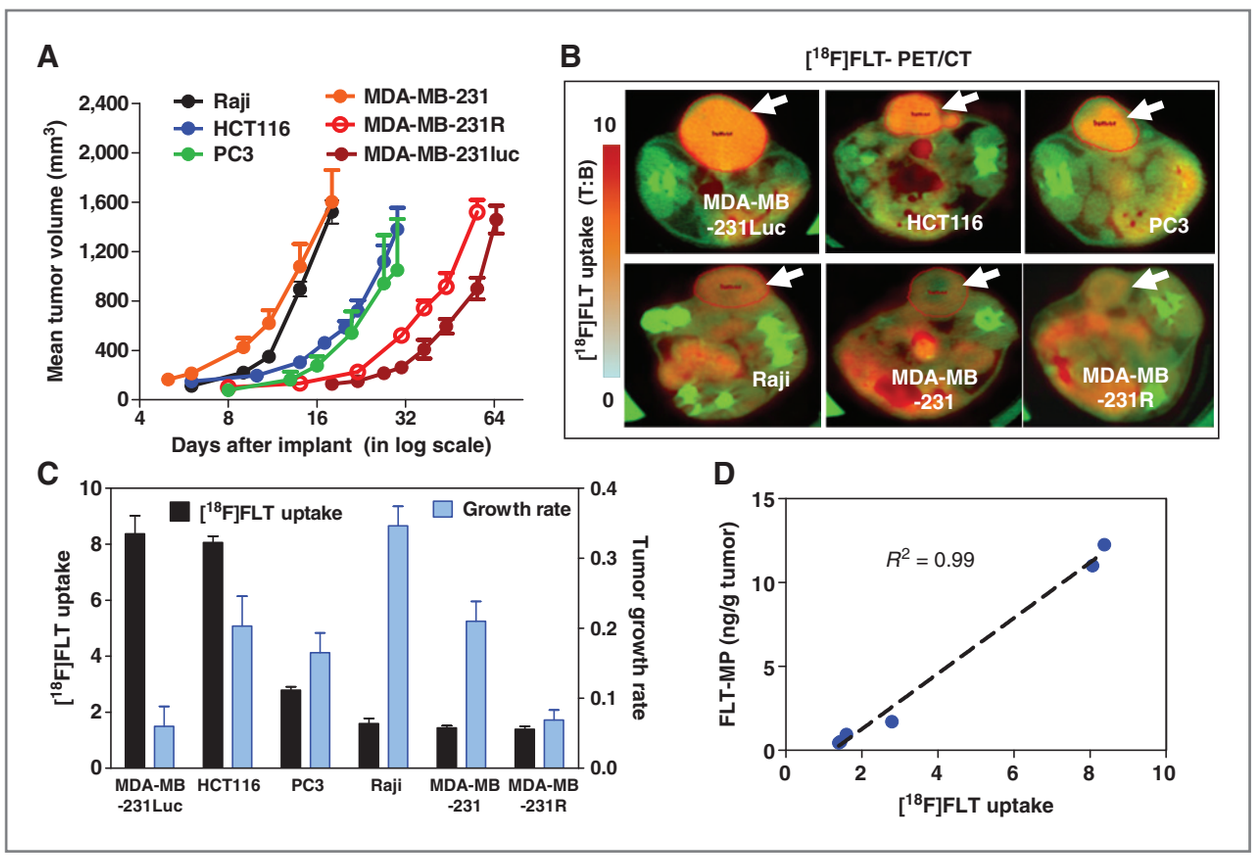

Figure 2. The correlation between tumor growth rate and [^{18}F]FLT tracer avidity in xenograft models. Values = mean ± SEM. The tumor growth curves (A) and representative images of [^{18}F]FLT–PET scans (B) of 6 xenograft tumor models. C, [^{18}F]FLT tracer avidity failed to reflect the tumor growth rate in tested xenografts. D, a linear correlation was observed between the radiotracer [^{18}F]FLT uptake and the FLT-MP level. In C and D, [^{18}F]FLT uptake = SUV ratio (tumor SUV_{max}/liver SUV_{mean}).

the cytoplasmic TK1- and Ki67-labeled cells did not show such a relationship (Fig. 3A and B). Given that Ki67 is also expressed during other non-S phases, with the exception of G_0, we expected that the fraction of Ki67-positive cells does not necessarily reflect the cell proliferation state of these tumor models. A distinctive feature of the TK1 staining was that in addition to the tumor cell cytoplasm, the interstitial space was positive for TK1, which might be due to the constitutive release of thymidine kinase by the dead or dying tumor cells (24, 25).

During the pyrimidine salvage pathway, FLT enters tumor cells, along with circulating thymidine, via nucleoside transporters. Once inside the cells, FLT is phosphorylated by thymidine kinases. Using TaqMan analysis, we determined the baseline mRNA expression of 7 members of the main nucleoside transport proteins family in the xenograft models: CNT-1, 2, and 3 and ENT-1, 2, 3, and 4. No clear correlation was observed between the expression of the transporters and [18F]FLT tracer avidity (Fig. 3C).

[18F]FLT and BrdUrd tracer exposures in the xenograft proliferation assays

The [18F]FLT tracer is retained intracellularly following its phosphorylation by TK1, which also phosphorylates thymidine. It was reported that thymidine present in the plasma and tissues competes with [18F]FLT. This affects the absolute uptake of [18F]FLT by tumors (26). Likewise, the ratio of BrdUrd to thymidine is thought to be critical to the BrdUrd incorporation assay, as BrdUrd is also phosphorylated by TK1. Therefore, the plasma exposures of FLT and BrdUrd were assessed after the administration of FLT and BrdUrd, respectively. Because both assays were carried out at 2-hour posttracer injection, the tracer exposure was assessed for the $AUC_{0-2\ h}$ value.

FLT plasma exposure was assessed at 2 μg/kg, an estimated dose level used in preclinical [18F]FLT–PET imaging. The mean plasma $AUC_{0-2\ h}$ value was 2 ng*h/mL (Fig. 4A), which was markedly (~200-fold) lower than the intrinsic plasma thymidine exposure in either naive or tumor-

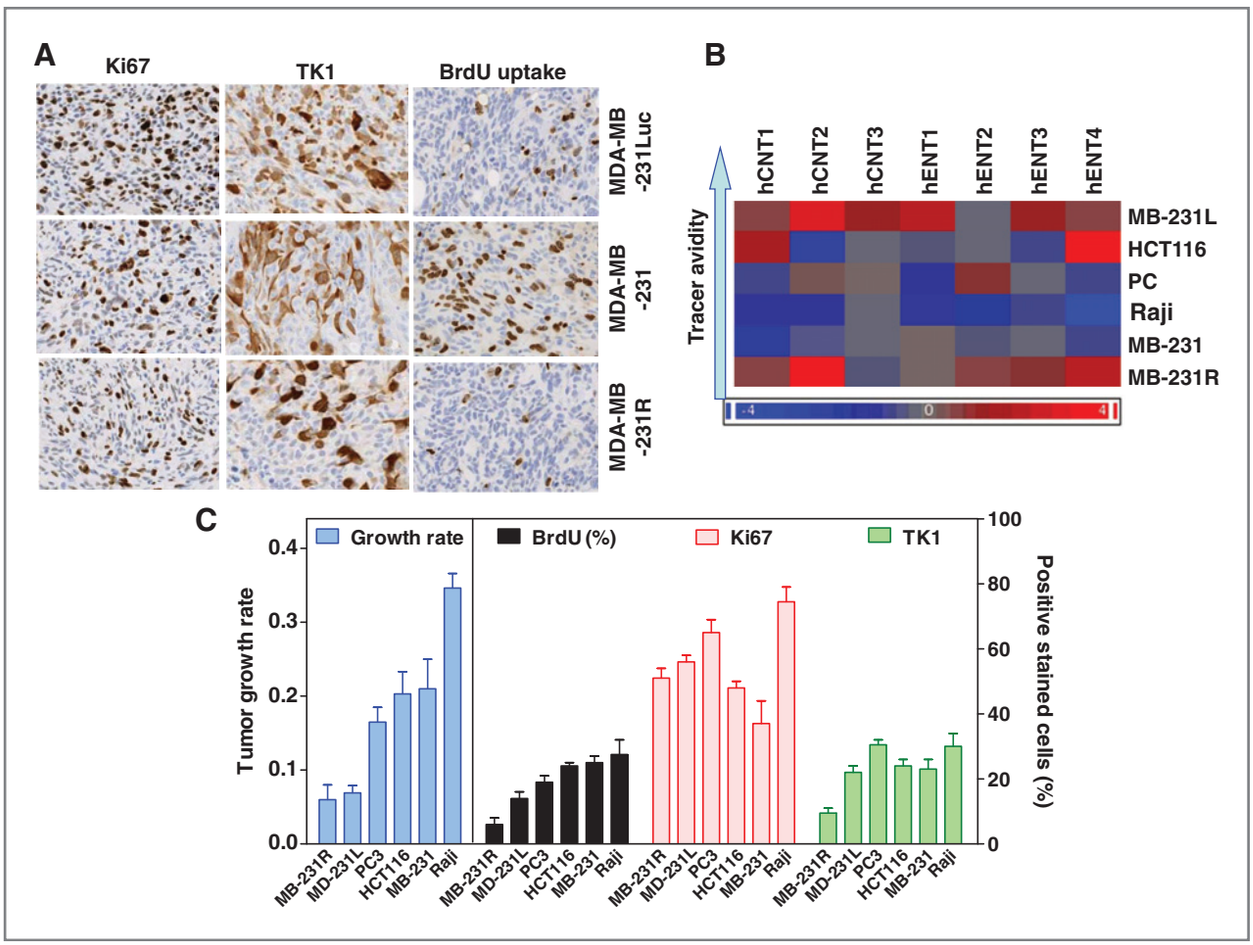

Figure 3. The correlation between tumor growth with histologic proliferation markers (Ki67, TK1, and BrdUrd) and the expression of nucleoside transporters in xenograft models. A, representative images of the MDA-MB-231Luc (high FLT tracer avidity), MDA-MB-231, and MDA-MB-231R models. B, the relative mRNA expression levels of nucleoside transporters in 6 tested xenografts. The expression of each was normalized to GAPDH, and relative mRNA expression was calculated by subtracting the average ΔC_t of triplicate reactions from the median of the average ΔC_t across cell lines. C, correlation of the tumor growth rate with the percentage of IHC positivity. Quantitative analysis of the IHC staining was carried out using a Vectra automated slide scanner.

bearing mice ($AUC_{0-2\ h}$ = 400 ng*h/mL). In contrast, BrdUrd at the 50 mg/kg dose level yielded an $AUC_{0-2\ h}$ of 1800 ng*h/mL, which was more than 4-fold higher than the thymidine $AUC_{0-2\ h}$.

In healthy human volunteers and cancer patients, plasma thymidine concentrations have been reported to be 320-fold lower than in rodents (27). We obtained similar results when analyzing the thymidine plasma levels from 10 healthy human volunteers. The mean $AUC_{0-2\ h}$ value for healthy volunteers was approximately 4.4 ng*h/mL (Thd = 2.5 ng/mL), whereas the estimated plasma $AUC_{0-2\ h}$ value for FLT was significantly lower (0.028 ng*h/mL) during [^{18}F]FLT–PET imaging for patients (28). The relative low exposure ratio of FLT to thymidine might be a limitation for the use of [^{18}F]FLT uptake as a surrogate measure for the cell proliferation status of tumors. To further investigate this hypothesis, we assessed whether FLT tracer uptake can truly reflect the thymidine salvage pathway when there are changes in local thymidine concentration.

Intrinsic tumor thymidine level negatively regulates FLT uptake

The intrinsic thymidine level in tumors was further assessed to correlate it with FLT tracer avidity in the tested models. Naive plasma and tumors (200–600 mm^3) were collected to assess thymidine level using LC/MS analysis. These tumor models exhibited variable levels of thymidine, despite having comparable plasma levels across all models (Supplementary Fig. S2). We observed an inverse relationship between the intrinsic tumor thymidine level and FLT tracer avidity (Fig. 4B). To further confirm the impact of intrinsic thymidine, miniosmotic pumps loaded with a solution of thymidine were subcutaneously implanted into HCT-116 tumor-bearing mice. A steady plasma level of thymidine was reached between 4 and 20 hours after pump implantation (data not shown). In the follow-up study, tumor-bearing mice were administered multiple doses of thymidine via the minipumps. Four hours after pump implantation, when plasma thymidine levels reached a steady state, FLT (2 μg/kg) was administered

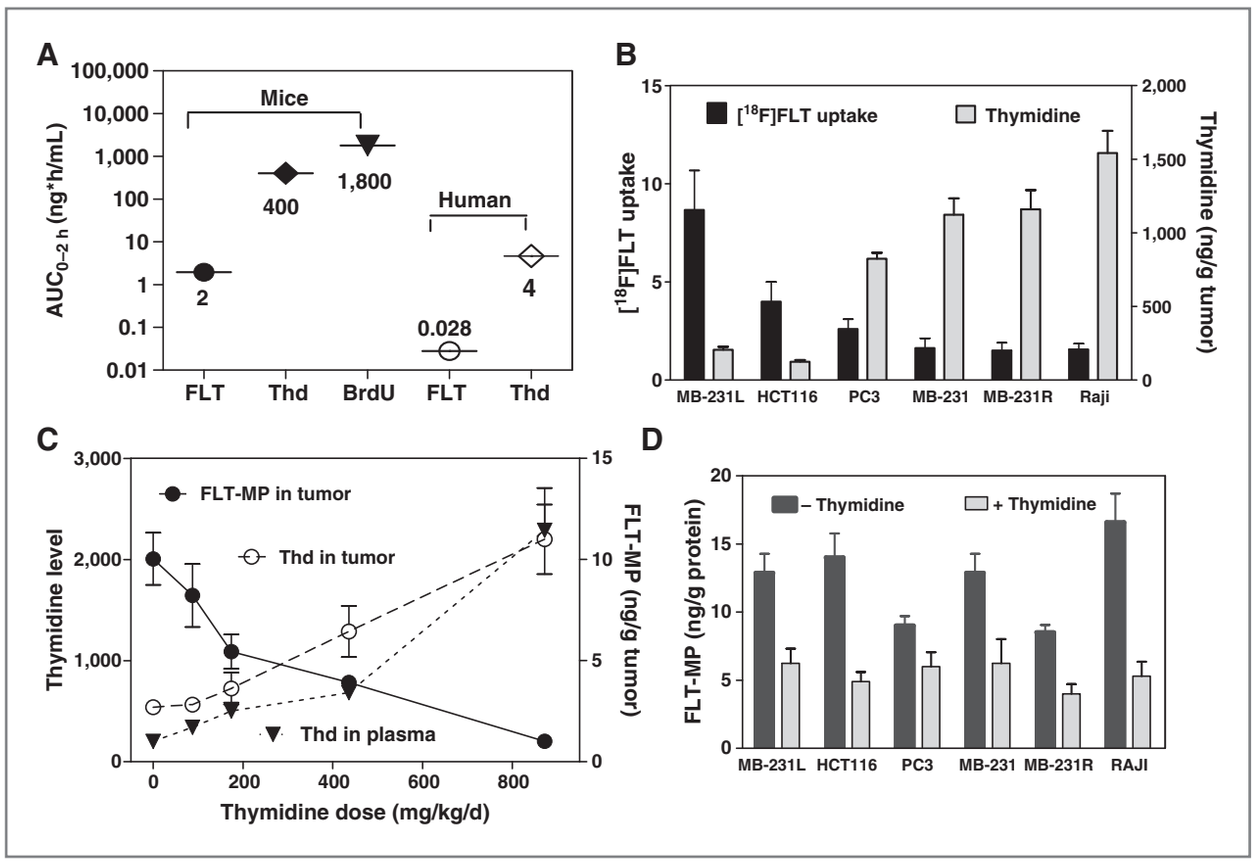

Figure 4. The effect of tracer exposure and thymidine levels on the FLT uptake and BrdUrd proliferation assay. A, plasma exposures ($AUC_{0-2\ h}$) of FLT, thymidine, and BrdUrd in mice and human during PET imaging or BrdUrd incorporation assay. B, [^{18}F]FLT uptake and the intrinsic tumor thymidine level showed an inverse relationship in the tested tumor models. [^{18}F]FLT uptake = SUV ratio (tumor SUV_{max}/liver SUV_{mean}. C, in the HCT116 tumor model, when thymidine exposure increased, FLT uptake (FLT-MP) decreased accordingly. Thymidine level is shown in ng/mL plasma or ng/10 g tumor. Thymidine was delivered via a subcutaneously implanted miniosmotic pump at 4 hours before FLT administration. D, *in vitro* assessment of FLT uptake (FLT-MP) in the presence and absence of thymidine (1 μmol/L).

intraperitoneally. Two hours after the injection of FLT, plasma and tumors were collected for pharmacokinetic analysis. As illustrated in Fig. 4C, when the thymidine levels in the plasma and tumors increased, the tumor FLT-MP levels decreased accordingly.

Similar results were observed in an *in vitro* setting when the corresponding tumor cell lines were used (Fig. 4D). Exponentially growing tumor cells were cultured with 100 nmol/L FLT in the presence and absence of 1 μmol/L thymidine. In all tested lines, the uptake of FLT, or the level of FLT-MP, was markedly reduced in the presence of thymidine. These results further showed that thymidine, at high concentrations, antagonizes the uptake of FLT by tumor cells.

PD-0332991 induces cell-cycle arrest in the G_1 phase, resulting in significant antitumor activity in the MDA-MB-231Luc tumor model

As a highly selective CDK4 inhibitor, PD-0332991 was reported to effectively arrest the cell cycle in the G_1 phase. We have used an Rb wild-type breast cancer cell line, MDA-MB-231Luc, for both the *in vitro* and *in vivo* tests. When MDA-MB-231Luc cells were treated with 1 μmol/L PD-0332991 for 24 hours, a significant induction of G_1 arrest (~87%) was observed (Fig. 5A) compared with nontreated cells (28%). After the removal of PD-0332991, cells become asynchronous in a time-dependent manner (Fig. 5B). When mice bearing established MDA-MB-231Luc tumors were treated with 150 mg/kg PD-0332991, using a dosing schedule of peroral administration daily for 15 days, a significant inhibition of tumor growth was observed with a TGI value of 98% and a median growth delay of 25 days.

Monitoring the PD-0332991 treatment-induced antiproliferative activity via immunohistochemical analyses and [18F]FLT–PET imaging

To assess the pharmacologic relevance of the PD-0332991–induced efficacy, mice with established MDA-MB-231Luc tumors were perorally administered 150 mg/kg PD-0332991 for 2 consecutive days. Twenty-four hours after the last treatment, mice were administered 50 mg/kg BrdUrd intraperitoneally for 2 hours. Tumors were harvested at the indicated times for IHC analysis. Consistent with previous findings, treatment of PD-0332991 resulted in Rb (Ser780) hypophosphorylation, which is indicative of the inhibition of its target, CDK4/6 (Fig. 6A and B). PD-0332991 concurrently caused a time-dependent decline in BrdUrd, TK1, and Ki67 IHC staining. These results suggested that the antiproliferative activity of PD-0332991 is the downstream effect of blocking CDK4.

In a separate cohort of tumor-bearing mice, the antiproliferative activity of PD-0332991 was further evaluated using [18F]FLT–PET imaging. Figure 6 depicts representative PET and CT images from each group 24 hours after the removal of the drug (C) and the quantitative analyses (D) of the time course for [18F]FLT uptake. Mice treated with PD-0332991 displayed a profound reduction in [18F]FLT uptake compared with the vehicle-treated group, suggesting

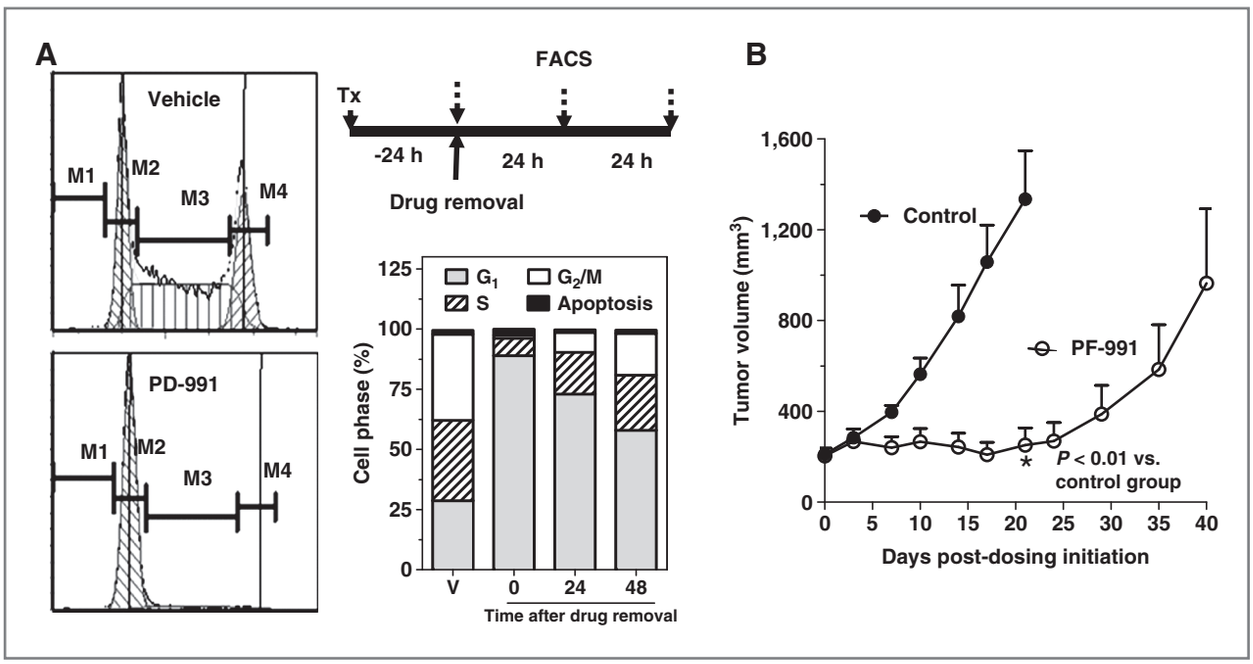

Figure 5. *In vitro* and *in vivo* antiproliferative activity of PD-0332991. A, MDA-MB-231Luc cells were treated with 1 μmol/L PD-0332991 for 24 hours. Cells were then harvested at the indicated time for cell-cycle analysis. Inhibition of CDK4/6 by PD-0332991 caused G_1 arrest, and the cells gradually returned to an asynchronous state after the drug removal. B, PD-0332991 exhibits antitumor activity in the MDA-MB-231Luc tumor model. PD-0332991 was perorally administered once daily for 14 days.

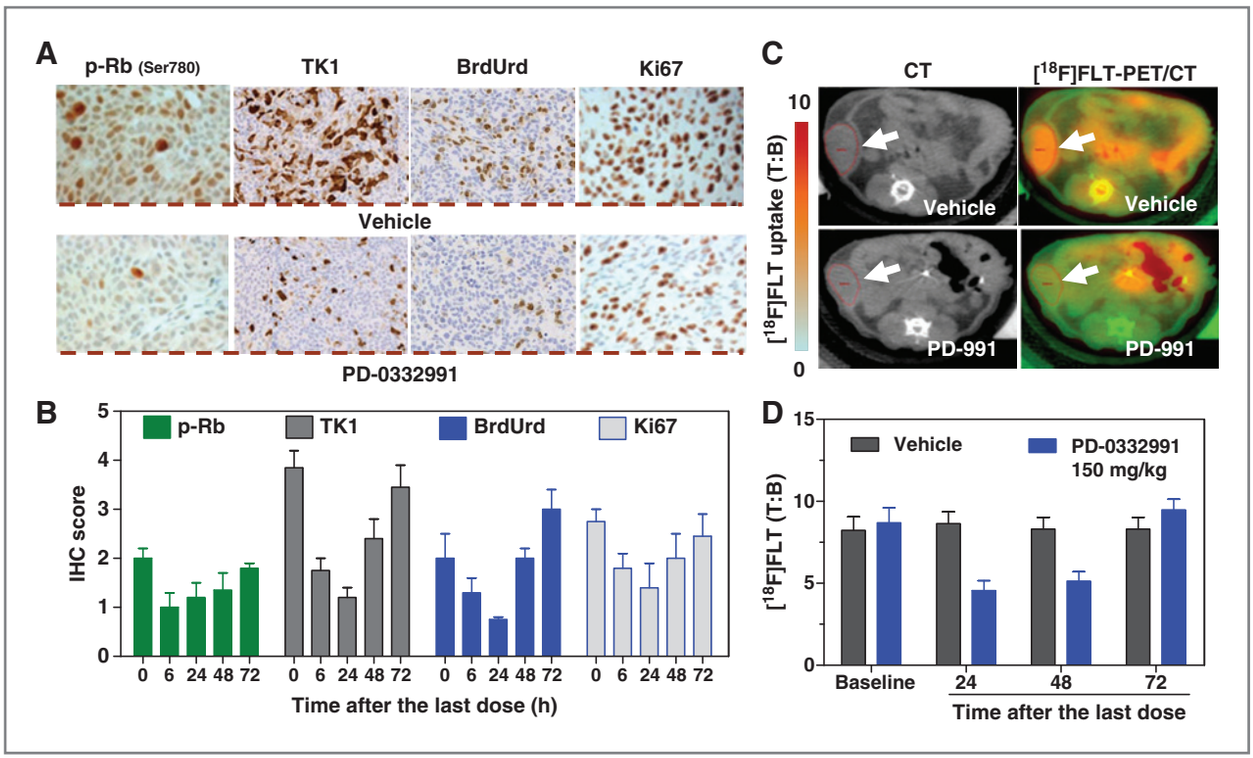

Figure 6. [^{18}F]FLT–PET/CT imaging and histologic analysis shows the target inhibition and antiproliferative effect of PD-0332991 in the MDA-MB-231Luc model. Mice bearing palpable tumors were perorally administered with 150 mg/kg PD-0332991 once daily for 2 days, and the tumors were harvested at the indicated times after the last dose for pharmacodynamic analysis. Representative images of phospho-Rb (Ser780), TK1, BrdUrd, Ki67 (A), CT and [^{18}F]FLT–PET imaging (B) at 24 hours after the last dose. The semiquantitative analyses of the IHC markers (C) and the quantitative analyses of [^{18}F]FLT uptake (D) in the tumor at the indicated time points after the last dose. The IHC staining was scored (0–4) by board-certified pathologists. [^{18}F]FLT uptake = SUV ratio (tumor SUV_{max}/liver SUV_{mean}). Values = mean ± SEM.

that the [^{18}F]FLT–PET imaging readout reflects either the antiproliferative activity or S-phase reduction of PD-0332991. Seventy-two hours after the drug removal, the antiproliferative activity was no longer measurable by IHC or PET imaging due to drug clearance and the return of cells to an asynchronous state. Clearly, the treatment-induced antiproliferative responses measured by the [^{18}F]FLT–PET imaging and histologic analyses of the proliferation markers were highly consistent.

Discussion

We examined whether [^{18}F]FLT–PET imaging can truly measure tumor cell proliferation in the preclinical setting. Parallel histologic assessments of other proliferation markers were carried out for comparison. More importantly, we evaluated factors other than cell proliferation that could impact the interpretation of the [^{18}F]FLT–PET imaging readout. This work provides practical insights into the most advantageous applications of [^{18}F]FLT–PET imaging in the oncology arena.

After being transported into cells by the nucleoside transporters, FLT or thymidine is phosphorylated by TK1 and retained in the proliferating cells, thus [^{18}F]FLT–PET imaging provide a surrogate measure of early-stage DNA salvage pathway. In this article, we validated the strong correlation between the [^{18}F]FLT tracer avidity and the uptake of [^{3}H]thymidine. Although ENT1, ENT2, CNT1, and CNT2 were reported to be responsible for FLT uptake in some tumor cell lines (3), we were unable to observe a positive correlation between the mRNA expression of 7 key nucleoside transporters and FLT tracer avidity in the tested panel of tumors. As a principal enzyme involved in the DNA salvage pathway, TK1 is more highly expressed in tumor cells than in normal nonproliferating cells (29, 30). Indeed, we observed strong cytosolic staining of TK1 in most of the growing xenografts, with the exception MDA-MB-231R. However, not all tumors with high TK1 levels "lit up" during [^{18}F]FLT–PET scan. In some rapidly growing tumors, including Raji and MDA-MB-231 models, poor FLT retention was observed despite the high expression of TK1. In conclusion, in order for FLT retention to be reflective of tumor cell proliferation, other factors may come into play besides the expressions of transporters and TK1.

Another determinant for [^{18}F]FLT uptake is the relative contribution of salvage pathway or *de novo* pathway to supply thymidine during DNA synthesis or cell

proliferation. Proliferating cells only take FLT or thymidine when cells primarily rely on the salvage pathway as a dominant source for DNA synthesis. In the work by Moroz and colleagues (7), *in vitro* assessment showed an 8-fold difference in the accumulation rates of [3H]FLT in HCT116 and SW620 cells, despite a small difference in their doubling time. *In vivo*, SW620 tumor model showed a considerably lower FLT avidity (37-fold) compared with that of HCT116 tumor due to a higher dependency on the *de novo* pathway of thymidine utilization. In contrast, our study results showed that the amount of FLT uptake, assayed by FLT-MP, was in the similar range via *in vitro* test, suggesting similar contributions of salvage pathway in the tested lines. In addition, BrdUrd incorporation significantly correlated with the tumor growth rate in the tested models. These results further confirmed that the disconnection between FLT uptake and tumor growth rate was not due to a lower cellular dependency on the salvage pathway, as BrdUrd uptake also reflects the salvage pathway of DNA synthesis.

In all tested lines, elevated level of thymidine significantly antagonized the FLT tracer uptake. *In vivo*, this inverse relationship between the plasma or tumor thymidine levels and tumor FLT uptake (FLT-MP) was confirmed by delivering variable concentrations of thymidine using miniosmotic pumps. Conversely, increased FLT uptake was observed by increasing the FLT dose (Supplementary Fig. S3). During [18F]FLT–PET imaging, the tracer is injected at a very low mass dose level to avoid any potential adverse effect. Using the FLT dosage in the preclinical [18F]FLT–PET imaging settings, the plasma exposure ($AUC_{0-2\ h}$) ratio of FLT to thymidine was shown to be 1 to 200. By comparison, BrdUrd injection, an alternative preclinical tool for S-phase assessment, resulted in a 4-fold higher exposure than thymidine. Compared with [18F]FLT–PET imaging, BrdUrd incorporation seems to be a more reliable predictive marker of proliferation because the high ratio of BrdUrd to thymidine alleviated the antagonistic action of thymidine. Our results provide an explanation for the lower FLT tracer avidities observed in some rapidly growing tumors, despite the high tumor proliferation rate. Raji and MDA-MB-231 tumors exhibited a considerably higher intrinsic thymidine level, thus thymidine uptake predominates over FLT tracer uptake. In comparison, the local thymidine level in the tracer-avid models, such as HCT116 and MDA-MB-231Luc, was nearly 100-fold less than that of Raji or MDA-MB-231 models.

This limitation could also apply in the clinical settings, in which the plasma $AUC_{0-2\ h}$ value of FLT is estimated to be nearly 150-fold less than thymidine (27, 28). The low ratio of exogenous tracer versus endogenous thymidine may explain why [18F]FLT–PET imaging is not appropriate for clinical tumor staging: proliferating tumors with high thymidine levels do not take up measurable level of FLT. In some cases, FLT exposure may be inconsistent between the baseline and after therapeutic treatment due to drug–drug interaction. In a preclinical study with sunitinib, the interpretation of [18F]FLT–PET imaging results was hampered by decreased plasma FLT exposure in treated mice (data not shown). Coupled with this finding, it was also suggested that FLT delivery can potentially be affected by other factors, such as changes in vascular permeability and perfusion after treatment (9). Because it is uncommon to consider background normalization for data analysis in the clinical setting, the exposure and biodistribution of FLT, as an exogenously injected tracer, could be a contributing factor that leads to false readout for [18F]FLT–PET imaging.

Early enthusiasm for the clinical utility of [18F]FLT uptake for tumor staging has faded, largely due to the overall lower tracer uptake and lower specificity in tumors compared with [18F]FDG uptake. In recent years, the primary application for this imaging modality has been focused on monitoring the therapeutic response after chemo- and targeted therapies, especially for targets that are strongly associated with cell-cycle inhibition (9). The study design often requires preselection of patients with higher tracer-avid lesions to allow for changes to be measured following therapy. As baseline scan for each patient can serve as his (her) own control, therefore the changes in FLT retention prior to and following treatment could provide clinical significance. One of the successful clinical applications of [18F]FLT–PET was the proof of mechanism study for a CDK4/6 inhibitor, PD-0332991. PD-0332991 induces cell-cycle arrest at the G_1 phase by inhibiting Rb (Ser780) phosphorylation. Clinically, treatment-induced cytostatic response was better reflected by the uptake of [18F]FLT than by [18F]FDG uptake in mantle cell lymphoma patients (17).

A preclinical [18F]FLT–PET imaging study was done to measure the treatment response of PD-0332991 using the MDA-MB-231Luc model. PD-0332991 caused the cells to arrest in G_1 and exhibited significant antitumor activity (TGI of 98%) *in vivo*. The biologic relevance of this study was shown by the modulation of phospho-Rb (Ser780) at the efficacious dose level of PD-0332991. Concurrently, PD-0332991 treatment induced a robust decline in [18F]FLT uptake after a short duration of treatment, with negligible impact on FLT tracer exposure. The [18F]FLT–PET imaging outcome correlated with histologic changes of proliferation markers, including positively stained Ki67 and TK1 cells, as well as BrdUrd incorporation. Furthermore, the early assessment of [18F]FLT uptake suppression occurred far before the treatment-induced change in tumor size became measurable. This preclinical validation strongly supports the clinical utility of [18F]FLT–PET imaging in confirming the proof of mechanism for the CDK4/6 inhibitor PD-0332991.

Correlating the modulation of target-associated biomarkers with therapy underscores the key objective of personalized medicine. Therefore, [18F]FLT–PET imaging might not be sufficient to serve as a standalone biomarker for clinical proof of mechanism. The advantage of [18F]FLT–PET imaging is to survey the entire patient malignancy noninvasively, thus avoiding sampling errors that can occur during a biopsy, particularly in heterogenic tumors. Unfortunately, 100% predictive biomarkers may be unrealistic to generate. The proof of mechanism study for PD-0332991 provided a good example of biomarker strategy. Pairing

the IHC measurement of target modulation with the decrease in [^{18}F]FLT uptake offered a robust measure for proof of mechanism and led to confidence in early therapy measurements.

Overall, our work provides some practical insights into the strengths and limitations of [^{18}F]FLT–PET imaging for oncology applications. With careful validation, [^{18}F]FLT–PET imaging technology might be considered for a wide variety of clinical applications, particularly in tracking antiproliferative therapies.

Disclosure of Potential Conflicts of Interest

All authors except C. Cullinane are Pfizer employees and shareholders.

Grant Support

C. Cullinane received research funding from Pfizer.

The costs of publication of this article were defrayed in part by the payment of page charges. This article must therefore be hereby marked *advertisement* in accordance with 18 U.S.C. Section 1734 solely to indicate this fact.

Received June 3, 2011; revised November 10, 2011; accepted November 28, 2011; published OnlineFirst December 14, 2011.

References

1. Shields AF, Grierson JR, Dohmen BM, Machulla HJ, Stayanoff JC, Lawhorn-Crews JM, et al. Imaging proliferation *in vivo* with [^{18}F]FLT and positron emission tomography. Nat Med 1998;4:1334–6.
2. Been LB, Suurmeijer AJH, Cobben DCP, Jager PL, Hoekstra HJ, Elsinga PH. [^{18}F]FLT-PET in oncology: current status and opportunities. Eur J Nucl Med Mol Imaging 2004;31:1659–72.
3. Paproski RJ, Ng AML, Yao SYM, Graham K, Young JD, Cass CE. The role of human nucleoside transporters in uptake of 3′-deoxy-3′-fluorothymidine. Mol Pharmacol 2008;74:1372–80.
4. Paproski RJ, Wuest M, Jans H-S, Graham K, Gati WP, McQuarrie S, et al. Biodistribution and uptake of 3′-deoxy-3′-fluorothymidine in ENT1-knockout mice and in an ENT1-knockdown tumor model. J Nucl Med 2010;51:1447–55.
5. Rasey JS, Grierson JR, Wiens LW, Kolb PD, Schwartz JL. Validation of FLT uptake as a measure of thymidine kinase-1 activity in A549 carcinoma cells. J Nucl Med 2002;43:1210–7.
6. Cole P, Smith A, Kamen B. Osteosarcoma cells, resistant to methotrexate due to nucleoside and nucleobase salvage, are sensitive to nucleoside analogs. Cancer Chemother Pharmacol 2002;50:111–6.
7. Moroz MA, Kochetkov T, Cai S, Wu J, Shamis M, Nair J, et al. Imaging colon cancer response following treatment with AZD1152: A preclinical analysis of [18F]Fluoro-2-deoxyglucose and 3′-deoxy-3′-[18F]fluorothymidine imaging. Clinical Cancer Res 2011;17:1099–110.
8. Mankoff DA, Eary JF. Proliferation imaging to measure early cancer response to targeted therapy. Clin Cancer Res 2008;14:7159–60.
9. Weber WA. Monitoring tumor response to therapy with 18F-FLT PET. J Nucl Med 2010;51:841–4.
10. De Saint-Hubert M, Brepoels L, Mottaghy FM. Can evaluation of targeted therapy in oncology be improved by means of 18F-FLT? J Nucl Med 2010;51:1499–500.
11. Solit DB, Santos E, Pratilas CA, Lobo J, Moroz M, Cai S, et al. 3′-Deoxy-3′-[18F]fluorothymidine positron emission tomography is a sensitive method for imaging the response of BRAF-dependent tumors to MEK inhibition. Cancer Res 2007;67:11463–9.
12. Ullrich RT, Zander T, Neumaier B, Koker M, Shimamura T, Waerzeggers Y, et al. Early detection of erlotinib treatment response in NSCLC by 3′-deoxy-3′-[18F]-fluoro-L-thymidine ([18F]FLT) positron emission tomography (PET). PLoS One 2008;3:e3908.
13. Aide N, Kinross K, Cullinane C, Roselt P, Waldeck K, Neels O, et al. 18F-FLT PET as a surrogate marker of drug efficacy during mTOR inhibition by everolimus in a preclinical cisplatin-resistant ovarian tumor model. J Nucl Med 2010;51:1559–64.
14. Zhang CC, Yan Z, Zhang Q, Kuszpit K, Zasadny K, Qiu M, et al. PF-03732010: A fully human monoclonal antibody against P-Cadherin with antitumor and antimetastatic activity. Clin Cancer Res 2010;16:5177–88.
15. Sohn H-J, Yang Y-J, Ryu J-S, Oh SJ, Im KC, Moon DH, et al. [18F]Fluorothymidine positron emission tomography before and 7 days after gefitinib treatment predicts response in patients with advanced adenocarcinoma of the lung. Clin Cancer Res 2008;14:7423–9.
16. Fry DW, Harvey PJ, Keller PR, Elliott WL, Meade M, Trachet E, et al. Specific inhibition of cyclin-dependent kinase 4/6 by PD 0332991 and associated antitumor activity in human tumor xenografts. Mol Cancer Ther 2004;3:1427–38.
17. Leonard JP, LaCasce A, Smith MR, Noy A, Yap JT, Van den Abbeele AD, et al. Cdk4/6 inhibitor PD 0332991 demonstrates cell cycle inhibition via FLT-PET imaging and tissue analysis in patients with recurrent mantle cell lymphoma. Blood 2008;112:264.
18. Li W, Araya M, Elliott M, Kang X, Gerk PM, Halquist MS, et al. Monitoring cellular accumulation of 3′-deoxy-3′-fluorothymidine (FLT) and its monophosphate metabolite (FLT-MP) by LC-MS/MS as a measure of cell proliferation *in vitro*. J Chromatogr B Analyt Technol Biomed Life Sci 2011;879:2963–70.
19. Grierson JR, Schwartz JL, Muzi M, Jordan R, Krohn KA. Metabolism of 3′-deoxy-3′-[F-18]fluorothymidine in proliferating A549 cells: Validations for positron emission tomography. Nucl Med Biol 2004;31:829–37.
20. Mehrara E, Forssell-Aronsson E, Ahlman H, Bernhardt P. Specific growth rate versus doubling time for quantitative characterization of tumor growth rate. Cancer Res 2007;67:3970–5.
21. Zhang C, Yan Z, Painter CL, Zhang Q, Chen E, Arango ME, et al. PF-00477736 mediates checkpoint kinase 1 signaling pathway and potentiates docetaxel-induced efficacy in xenografts. Clin Cancer Res 2009;15:4630–40.
22. Leyton J, Latigo JR, Perumal M, Dhaliwal H, He Q, Aboagye EO. Early detection of tumor response to chemotherapy by 3′-Deoxy-3′-[18F]fluorothymidine positron emission tomography: The effect of cisplatin on a fibrosarcoma tumor model *in vivo*. Cancer Res 2005;65:4202–10.
23. Brepoels L, Stroobants S, Verhoef G, De Groot T, Mortelmans L, De Wolf-Peeters C. 18F-FDG and 18F-FLT uptake early after cyclophosphamide and mTOR inhibition in an experimental lymphoma model. J Nucl Med 2009;50:1102–9.
24. Taylor A, Hewitt EG, Jones OW. Tumor-associated thymidine kinase in the sera of rats with transplanted hepatomas. Cancer Res 1976;36:2070–2.
25. Rehn S, Gronowitz JS, Källander C, Sundström C, Glimelius B. Deoxythymidine kinase in the tumour cells and serum of patients with non-Hodgkin lymphomas. Br J Cancer 1995 71:1099–105.
26. Barthel H, Cleij MC, Collingridge DR, Hutchinson OC, Osman S, He Q, et al. 3′-Deoxy-3′-[18F]fluorothymidine as a new marker for monitoring tumor response to antiproliferative therapy *in vivo* with positron emission tomography. Cancer Res 2003;63:3791–8.
27. Li KM, Clarke SJ, Rivory LP. Quantitation of plasma thymidine by high-performance liquid chromatography–atmospheric pressure chemical ionization mass spectrometry and its application to pharmacodynamic studies in cancer patients. Anal Chim Acta 2003;486:51–61.
28. Turcotte E, Wiens L, Grierson J, Peterson L, Wener M, Vesselle H. Toxicology evaluation of radiotracer doses of 3′-deoxy-3′-[18F]fluorothymidine (18F-FLT) for human PET imaging: Laboratory analysis of serial blood samples and comparison to previously investigated therapeutic FLT doses. BMC Nucl Med 2007;7:1–9
29. Boothman DA, Davis TW, Sahijdak WM. Enhanced expression of thymidine kinase in human cells following ionizing radiation. Int J Radiat Oncol Biol Phys 1994;30:391–8.
30. Salskov A, Tammisetti VS, Grierson J, Vesselle H. FLT: Measuring tumor cell proliferation *in vivo* with positron emission tomography and 3′-deoxy-3′-[18F]fluorothymidine. Semin Nucl Med 2007;37:429–39.